Dietary Sodium Intake Regulates the Ubiquitin-Protein Ligase Nedd4-2 in the Renal Collecting System

Dominique Loffing-Cueni,*‖ Sandra Y. Flores,* Daniel Sauter,† Dorothée Daidié,* Nicole Siegrist,† Pierre Meneton,‡ Olivier Staub,* and Johannes Loffing§

*Department of Pharmacology & Toxicology, University of Lausanne, Lausanne, Switzerland; †Institute of Anatomy, University of Zurich, Zurich, Switzerland; ‡Unité 652, Institut National de la Santé et de la Recherche Médicale, Paris, France; and Units of §Anatomy and ‖Histology, Department of Medicine, University of Fribourg, Fribourg, Switzerland

The activity of the epithelial sodium (Na^+) channel (ENaC) in the aldosterone-sensitive distal nephron (ASDN) needs to be tightly regulated to match urinary Na^+ excretion with dietary Na^+ intake. The ubiquitin-protein ligase Nedd4-2, which *in vitro* interacts with ENaC subunits and reduces ENaC cell surface abundance and activity by ubiquitylation of the channel, may participate in the control of ENaC. This study confirms *in vivo* by reverse–transcriptase–PCR that Nedd4-2 is expressed throughout the nephron and is detectable by immunoblotting in kidney extracts. By immunohistochemistry, Nedd4-2 was found to be strongly expressed in the ASDN, with low staining intensity in the late distal convoluted tubule and early connecting tubule (where apical ENaC is high) and gradually increasing detection levels toward the collecting duct (CD; where apical ENaC is low). Compared with high-Na^+ diet (5% Na^+), 2 wk of low-Na^+ diet (0.01% Na^+) drastically reduces Nedd4-2 immunostaining and increases apical ENaC abundance in ASDN. Reduced Nedd4-2 immunostaining is not dependent on increased apical Na^+ entry in the CD, because it is similarly observed in mice with intact and with suppressed apical ENaC activity in the CD. Consistent with a role of mineralocorticoid hormones in the long-term regulation of Nedd4-2, 5-d treatment of cultured CD ($mpkCCD_{cl4}$) cells with 1 μM aldosterone leads to reduction of Nedd4-2 protein expression. It is concluded that Nedd4-2 abundance is regulated by Na^+ diet, by a mechanism that likely involves aldosterone. This regulation may contribute to adaptation of apical ENaC activity to altered Na^+ intake.

J Am Soc Nephrol 17: 1264–1274, 2006. doi: 10.1681/ASN.2005060659

Renal sodium (Na^+) excretion has to match dietary Na^+ intake to maintain extracellular salt and volume homeostasis. The aldosterone-sensitive distal nephron (ASDN), which comprises late distal convoluted tubule (DCT, or DCT2 [1]), connecting tubule (CNT), and cortical and medullary collecting duct (CCD and MCD, respectively) (2), mediates the final control of renal Na^+ excretion (3,4). The Na^+ transport rate along this segment critically depends on the activity and abundance of the epithelial Na^+ channel (ENaC) in the luminal membrane. Consistently, ENaC is a main target by which hormones and other factors control the Na^+ transport in the ASDN (3,4).

Aldosterone profoundly stimulates ENaC activity and increases Na^+ transport in the ASDN and likely mediates many effects of altered Na^+ intake on renal Na^+ handling (for comprehensive reviews on ENaC regulation and/or aldosterone, action consult [3,4]). Exogenous aldosterone application and dietary Na^+ restriction (increasing endogenous aldosterone) similarly augment the number of active Na^+ channels in the luminal membrane of the ASDN, which involves a redistribution of all three ENaC subunits (α, β, and γ) from a cytoplasmic pool to the apical plasma membrane (2,5,6). The apical redistribution of ENaC shows a remarkable axial heterogeneity along the ASDN. It is most pronounced in the early ASDN portions (late DCT and early CNT) and progressively decreases along further downstream localized segments (late CNT and CD) (2,6). This morphologically ascertainable gradient is consistent with numerous functional studies showing several-fold higher transepithelial Na^+ transport rates and ENaC activity in the CNT than in the CD (7–11). However, the underlying molecular mechanisms for this axial heterogeneity are unclear.

An important pathway that controls the abundance and activity of ENaC in the apical plasma membrane involves the ubiquitin-protein ligase Nedd4-2, an intracellular enzyme that is known to interact with so-called PY motifs (xPPxY; x is any amino acid, P is proline, and Y is tyrosine) on the C-termini of each ENaC subunit (12–15). Nedd4-2 acts in concert with the ubiquitin-activating enzyme E1 and with the ubiquitin-activating enzyme UBE2E3 (16) to conjugate ubiquitin peptides on the N-termini of the ENaC subunits (17). Such ubiquitylated channels are internalized and sorted for degradation by lysosomal and proteasomal pathways (12,13,17). Moreover, recent evidence suggested that some of the ubiquitylated channels are

Received June 27, 2005. Accepted February 8, 2006.

Published online ahead of print. Publication date available at www.jasn.org.

Address correspondence to: Dr. Johannes Loffing, University of Fribourg, Department of Medicine–Anatomy, Route Albert Gockel 1, CH-1700 Fribourg, Switzerland. Phone: +41-26-300-8527; Fax: +41-26-300-9733; E-mail: johannes.loffing@unifr.ch

ISSN: 1046-6673/1705-1264

released *via* exosomes into the tubular lumen of the renal collecting system (18). In Liddle's syndrome, a rare form of monogenic hypertension, mutations in the β- or γ-ENaC genes delete the PY motifs (19,20). Recently, it was shown that the interaction between Nedd4-2 and ENaC is regulated by serum- and glucocorticoid-induced kinase 1 (Sgk1), a protein kinase whose expression is regulated by aldosterone and that is able to stimulate ENaC and transepithelial Na^+ transport (21–23). It is thought that aldosterone stimulates transepithelial Na^+ transport in part by increasing expression of Sgk1 and by phosphorylation of Nedd4-2. Nedd4-2 phosphorylation generates Nedd4-2 binding sites for 14-3-3 proteins, causing reduced Nedd4-2/ENaC interaction and consequently reduced ubiquitylation and accumulation of ENaC at the plasma membrane (24–28).

Notably, these concepts have been derived mainly from experiments in heterologous expression systems or cell lines as model systems for the ASDN. Little is known about the *in vivo* regulation of Nedd4-2. Previous studies addressed the short-term effect of aldosterone on Nedd4-2 in the CD but did not examine the more chronic effects of altered dietary Na^+ intake (24). In this study, we used two Nedd4-2–specific affinity-purified Nedd4-2 antisera, directed against different epitopes within Nedd4-2, to provide a comprehensive analysis of the distribution and regulation by dietary Na^+ intake of Nedd4-2 along the nephron.

Materials and Methods

Animal Experiments

Animal studies were in accordance with the Guide for Care and Use of Laboratory Animals (Institute of Laboratory Animal Resources, National Academy of Science, Bethesda, MD). Experiments were performed with 6- to 8-wk-old male NMRI mice (Iffa Credo, Arbresle, France), male Sprague Dawley rats (Harlan, Horst, Netherlands), and kidneys from previously described male $Scnn1a^{loxlox}$ and $Scnn1a^{loxloxCre}$ mice (29).

Series 1. Thirty NMRI mice (body weight between 25 and 30 g) were randomly divided in two groups of 15 mice each. Group 1 received for 2 wk a diet with high Na^+ contents (5.0%), whereas group 2 received a diet with low Na^+ (0.01%) contents (UAR, Epinay-S/Orge, France). During the last 4 d of the experiment, mice were housed individually in metabolic cages to record 24-h urinary volume and urinary Na^+ and K^+ excretion. Urinary Na^+ and K^+ concentrations were measured with an indirect potentiometer (Beckman model E2A, Villepinte/Orsy, France). Plasma levels of aldosterone were measured by RIA (Aldo RIA; Sanofi Diagnostics, Marnes-La-Coquette, France) in blood that was taken from the retrobulbar venous plexus under anesthesia with a combination of ketamine (Narketan 10, 80 mg/kg body wt; Chassot, Belp, Switzerland) and xylazine (Rompun, 33 mg/kg body wt; Bayer, Leverkusen, Germany).

Series 2. Ten Sprague Dawley rats (body weights between 200 and 220 g) were divided in two groups of five rats each and received either the standard diet (0.3% Na^+) or a low-Na^+ (0.01%) diet for 2 wk.

Series 3. Rubera *et al.* (29) generated by CreLox technology mice with targeted inactivation of α-ENaC specifically in the CD. Mice with "floxed" but intact α-ENaC alleles ($Scnn1a^{loxlox}$) are similar to wild-type mice. Mice with CD-specific α-ENaC deletion ($Scnn1a^{loxloxCre}$) lack any apical ENaC activity in the CD but are otherwise normal. The remaining ENaC activity in connecting tubules seems to be sufficient to keep the animals in Na^+ balance even when challenged by 6 d of Na^+ restriction (29). Kidneys of four $Scnn1a^{loxlox}$ and four $Scnn1a^{loxloxCre}$ mice that were kept on standard-Na^+ (0.3%) diet and four $Scnn1a^{loxlox}$ and five $Scnn1a^{loxloxCre}$ mice that were kept for 6 d on low-Na^+ (0.01%) diet were used for this study.

Reverse Transcriptase–PCR on Microdissected Tubules

Nephron segments were obtained by microdissection from three normal mice as described previously (30). After anesthesia (Nembutal, 5 mg/100 g body wt), the left kidney was perfused with collagenase that was dissolved in microdissection medium. Thin pieces of tissue were postincubated in the microdissection solution that contained collagenase (1 mg/ml). Glomeruli, proximal tubules (PT), medullary and cortical thick ascending limbs (mTAL and cTAL, respectively), and CCD were isolated. Total RNA were extracted from isolated glomeruli (5–10) and nephron segments (40 mm each) using a microtechnique (30) adapted from the method of Chomczynski and Sacchi (31). Reverse transcriptase (RT) was performed using Superscript II (Invitrogen, Carlsbad, CA) with 5× RT buffer (4 μl), 100 mM dithiothreitol (2 μl), 50 μM random hexamers (1 μl; Applied Biosystems, Foster City, CA), 20 mM dNTP (1 μl; GE Healthcare, Munich, Germany), H_2O (1 μl), and 10 μl of tubules RNA. For analysis of Nedd4-2 expression along the nephron, standard RT-PCR was carried out on total RNA from 1 mm of isolated nephron segments of three normal mice using the Titan one-tube RT-PCR system (Roche, Rotkreuz, Switzerland) with the following Nedd4-2 primers: Sense 5′-ccattctacaagatgatgctgggg-3′, antisense 5′-gctctattgtaaacagctgaggacc-3′; 35 cycles of PCR. Amplified DNA fragments were visualized on an agarose gel that was stained with ethidium bromide. For quantitative real-time RT-PCR (7500 Fast Real-Time PCR System; Applied Biosystems), reverse transcription was performed on total RNA from microdissected mouse CCD tubules, using Superscript II (Invitrogen). For the quantitative real-time PCR, a standard curve (five dilutions) was done with cDNA from $mpkCCD_{cl4}$ cells (32). The reaction was performed in a total volume of 20 μl according to the manufacturer's instructions; each reaction was done in triplicate. The primers were from Applied Biosystems, corresponding to the following order numbers: glyceraldehyde-3-phosphate dehydrogenase (mouse GAPDH), Mm99999915_g1; mSGK1, Mm00441380_m1; and mNedd4-2, Mm00459584_m1. The data were analyzed using the software provided with the instrument, and results were normalized to GAPDH and to the low-Na^+ condition.

Western Blot Analysis

For each mouse, 70 μg of protein extracts from homogenized renal cortex was separated by SDS-PAGE (7% polyacrylamide gels) and blotted on polyvinylidene difluoride membranes (Bio-Rad, Reinach, Switzerland). Membranes were blocked with dry milk (5%) in a Tris-NaCl-Tween buffer and incubated with either affinity-purified rabbit anti-mouse Nedd4-2 antisera A26 (24) diluted 1:500 or A27 (33) diluted 1:200. Bound Nedd4-2 antibodies were revealed with horseradish peroxidase–conjugated sheep anti-rabbit IgG (Amersham, Pharmaceutica, Otelfingen, Switzerland) followed by enhanced chemiluminescence (ECL; Amersham) and exposure to Biomax XAR films (Kodak, Rochester, NY). Subsequently, blots were exposed to mouse anti–β-actin antibodies (Sigma, St. Louis, MO; dilution 1:5000) and horseradish peroxidase–conjugated goat anti-mouse IgG (Amersham). Signal intensities of recognized Nedd4-2–related bands were quantified using a molecular imager FX (Bio-Rad, Hercules, CA) and normalized to the β-actin control. In competition experiments, the primary antibodies were preincubated with the GST fusion proteins (100 μg/ml) that were used for the immunization of the rabbits.

Immunohistochemistry

The kidneys of anesthetized mice and rats were fixed by vascular perfusion with 3% paraformaldehyde/0.05% picric acid and processed for immunohistochemistry as described previously (6). Serial cryosections (4 μm thick) were incubated with one of the following primary antibodies: Affinity-purified rabbit anti-mouse Nedd4-2 (A26; [24]) diluted 1:500, affinity-purified rabbit anti-mouse Nedd4-2 (A27 [33]) diluted 1:200, rabbit anti-rat α-ENaC diluted 1:500 (29), rabbit anti-rat β-ENaC diluted 1:500 (29), mouse anti-bovine H-ATPase diluted 1:4 (34), or mouse anti-chicken calbindin D28K diluted 1:20,000 (Swant, Bellinzona, Switzerland). The binding sites of the primary antibodies were revealed by Cy3-conjugated goat anti-rabbit IgG (Jackson ImmunoResearch Laboratories, West Grove, PA) and FITC-conjugated goat anti-mouse Ig (Jackson ImmunoResearch Laboratories) diluted 1:1000 and 1:40, respectively. All antibody dilutions were in PBS-1% BSA. The specificity of the Nedd4-2 antibodies was confirmed by preincubations with the GST fusion proteins (100 μg/ml) that had been used for the immunization of the rabbits.

Evaluation of Immunofluorescence

The sections were studied with a Zeiss fluorescence microscope by three investigators (D.L.C., D.S., and J.L.), who were blinded to the treatment or genotype of the animals. Tubular segments were identified according to standard morphologic criteria. CNT and CCD were distinguished on the basis of their localization in the cortical labyrinth and in the medullary rays, respectively. Qualitative judgments regarding immunostainings were similar for all investigators. For further confirmation of qualitative ratings about Nedd4-2 immunofluorescent intensities, micrographs of the stained cryosections were taken and analyzed by determining the mean pixel intensities (MPI) in at least three randomly selected CCD profiles of each animal. MPI were determined with National Institutes of Health Imaging software, normalized to the background fluorescence in nuclei of PT, and expressed in arbitrary units as described previously (24)

Cell Culture

Experiments were carried out in the mpkCCD$_{c14}$ cell line, a clone of principal cells that has been derived from microdissected CCD of an SV-PK/Tag transgenic mouse (32). Cells were cultured on plastic tissue-culture flasks as described previously (35). For studying the effect of aldosterone on Nedd4-2 expression, cells were grown on collagen-coated filters (Transwell 0.4-μm pore, 4.7 cm^2). At confluence, cells were maintained in modified Ham's F12 medium without EGF, transferrin, and FCS. Cells then were kept for 5 d in the presence of vehicle or 1 μM aldosterone. The medium was replaced daily, and fresh aldosterone was added. Cells were lysed in lysis buffer (50 mM HEPES [pH 7.5], 150 mM NaCl, 1.5 mM $MgCl_2$, 1 mM EGTA, 10% glycerol, and 1% Triton X-100) that contained protease inhibitors (1 mM PMSF, 10 μg/ml leupeptin, 10 μg/ml pepstatin A, and 10 μg/ml aprotinin). Samples were analyzed by SDS-PAGE/Western blotting as described above.

Statistical Analyses

The data are given as means ± SEM. Statistical differences between means of groups were evaluated by *t* test or by ANOVA followed by Bonferroni multiple comparisons test using standard computer software. Differences were considered statistically significant at $P > 0.05$.

Results

Effect of Na^+ Diets on Urinary Na^+ and K^+ Excretion and Plasma Levels of Aldosterone

To establish experimental conditions in which to study the influence of Na^+ diet on Nedd4-2 expression, we confirmed first the effect of Na^+ diets on urinary Na^+ and K^+ excretion and on plasma levels of aldosterone. Mice were kept either on a high (5% Na^+) or a low (0.01% Na^+) dietary Na^+ intake. After 2 wk on the dietary regimens, urinary Na^+ and K^+ excretion was determined by urine sampling during the last 24-h period. Mice with high dietary Na^+ intake excreted significantly higher amounts of Na^+ (2935 ± 179 μmol Na^+/d; $n = 15$ mice) and water (9.75 ± 1.31 ml/d water; $n = 15$ mice) than mice that fed a low-Na^+ diet (12 ± 5 μmol Na^+/d; 1.01 ± 0.46 ml/d water; $n = 15$ mice). The high water excretion on high Na^+ intake is likely explained by salt-induced thirst. The urinary K^+ excretion was not affected (372 ± 28 [high Na^+] *versus* 368 ± 37 μmol/d K^+ [low Na^+]; $n = 15$ mice per group). In mice that were fed for 2 wk the high-Na^+ diet, the plasma level of aldosterone was 46.4 ± 3.5 pg/ml (approximately 0.1 nM), and in mice that were fed for 2 wk the low-Na^+ diet, the level was 414.7 ± 23.7 pg/ml (approximately 1.0 nM).

Detection of Nedd4-2 mRNA in Microdissected Nephron Portions

Previous studies on rat (24) and human (36) kidneys indicated that Nedd4-2 is expressed in several nephron portions. To confirm these observations for mouse kidneys, we performed RT-PCR experiments on microdissected tubules from mice ($n = 3$) that were on the standard-Na^+ diet (0.8% Na^+). Nedd4-2 mRNA expression was found in PT, mTAL and cTAL, and CCD (Figure 1). The strongest signals for Nedd4-2 mRNA were seen in samples from PT and CCD. The signal intensities of samples from mTAL and cTAL were usually less intense and for mTAL often close to the detection limit (see Figure 1). Nedd4-2 mRNA was not detectable in microdissected glomeruli.

Characterization of Nedd4-2 Antibodies on Mouse Tissue Samples

For Western blot analysis and immunohistochemistry, we used affinity-purified antisera A26 (24) and A27 (33) that were raised against different epitopes and that specifically recognize

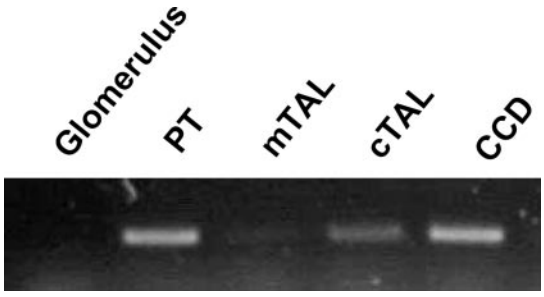

Figure 1. Detection of Nedd4-2 mRNA in microdissected nephron portions from mouse kidney. Glomeruli, proximal tubules (PT), medullary and cortical thick ascending limbs (mTAL and cTAL, respectively), and cortical collecting ducts (CCD) were microdissected from murine kidney; RNA was isolated; and reverse transcriptase–PCR (RT-PCR) was performed using primers specific for Nedd4-2 as described in Materials and Methods. The amplified fragments were verified by sequencing.

mouse Nedd4-2 but not Nedd4 (33). In Western blot analysis of mouse kidney cortex homogenates, both antibodies showed similar binding patterns with one major band at approximately 120 kD and several additional bands at lower molecular weights (Figure 2). The multiple bands likely reflect the expression of several Nedd4-2 variants as a result of alternative promoters and splicing (37–39). Alternative promoters and splicing also may explain the slight differences in the banding patterns between both antibodies, because the antibodies recognized different epitopes, which are not necessarily present in all Nedd4-2 variants. Preincubation of the antibodies with the Nedd4-2 GST fusion protein that was used for immunization completely abolished the binding of the antibody to the membrane (Figure 2).

In immunohistochemical experiments, both anti–Nedd4-2 antibodies showed similar binding patterns with a strong cytoplasmic labeling in CD profiles. Preincubation of the antibodies with the corresponding but not with the noncorresponding Nedd4-2 GST fusion protein abolished the immunostaining (Figure 3A). Compared with ASDN segments, PT and distal tubules revealed weak Nedd4-2–related immunostaining,

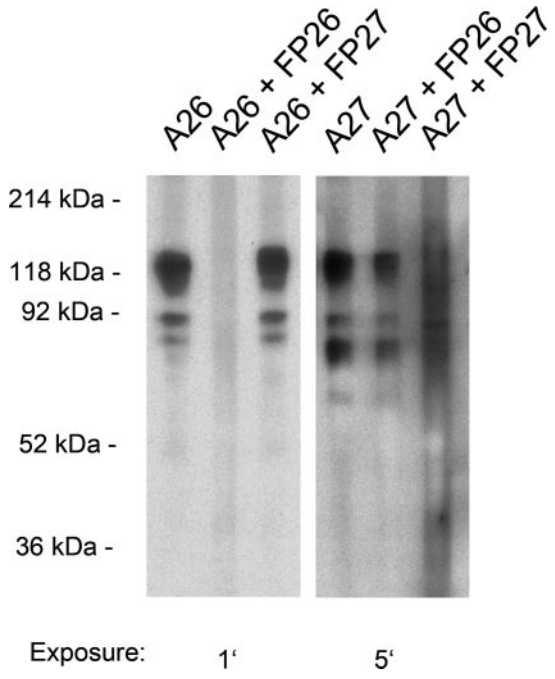

Figure 2. Characterization of affinity-purified anti–Nedd4-2 antisera A26 and A27 by Western blot analysis. Homogenates of kidney cortex of normal mice (700 μg of protein loaded per gel in a single wide slot) were subjected to SDS-PAGE analysis and transferred to polyvinylidene difluoride membrane. Using the multiscreen apparatus of BioRad, separated lanes on the same membrane were incubated with affinity-purified anti–Nedd4-2 antisera A26 and A27 as indicated. Preincubation of the affinity-purified antisera with the corresponding fusion protein that was used for immunization (FP26 and FP27, respectively) abolished the specific binding of the antisera to the membrane. The left (A26) and right (A27) halves of the same membrane are shown at different exposure times for enhanced chemiluminescence detection.

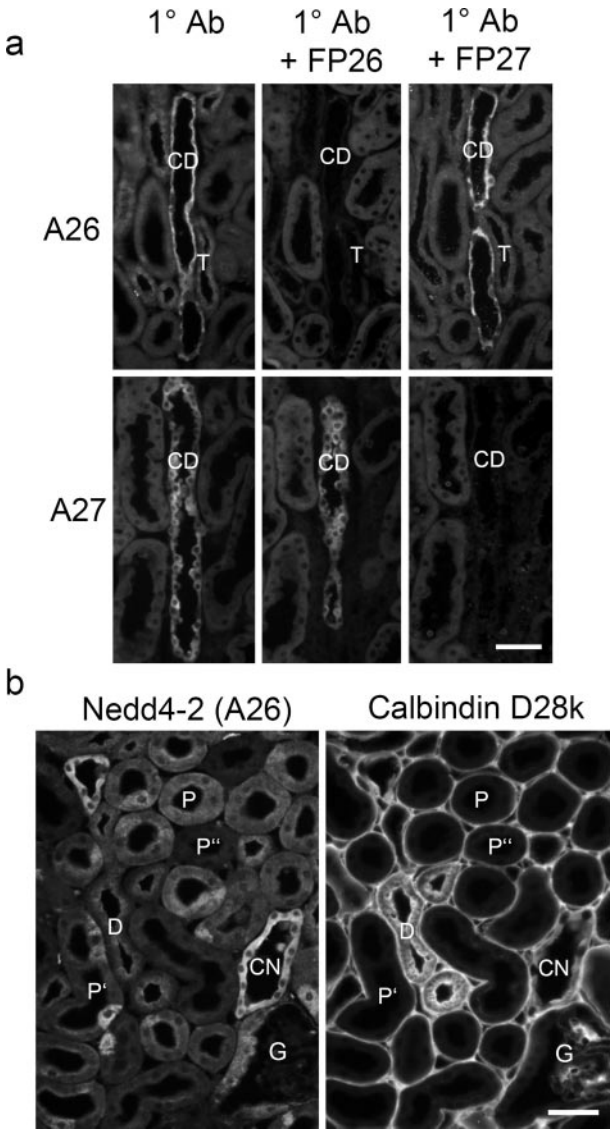

Figure 3. (A) Medullary rays in mouse renal cortex. Immunostaining for Nedd4-2 with affinity-purified antisera A26 (diluted 1:500) and A27 (dilution 1:200) shows a strong cytoplasmic staining in CD. Weak immunostaining also is seen in adjacent thick ascending limb (T). Preincubation of the affinity-purified antisera with the corresponding fusion protein that was used for immunization (FP26 and FP27, respectively) abolished the specific binding of the antisera to the section. Each row shows consecutive cryosections. (B) Cortical labyrinth of mouse kidney. Co-immunostaining with affinity-purified antiserum A26 (diluted 1:300) and mouse anti-calbindin D28k (CB; diluted 1:20,000). Nedd4-2 is seen in CB-positive distal convoluted tubules (D) and connecting tubules (CN), as well as in CB-negative proximal tubules (P). The presence of CB-negative intercalated cells (IC) and the slightly weaker CB staining distinguishes the CN from D. Note the diffuse intracellular localization of Nedd4-2 in the cytoplasm of CN and most P and the more subapical localization of Nedd4-2 in D and few P. Nedd4-2 immunostaining in profiles of P is heterogeneous and ranges from strong labeling of all epithelial cells (P), *via* labeling of only single cells (P′) to very weak immunostaining (P″). The strong immunofluorescent labeling of tubular basement membranes and interstitial cells in the right panel of B (calbindin D28k) is due to binding of the secondary FITC-labeled anti-mouse IgG to endogenous immunoglobulins. Bar = approximately 50 μm.

which became clearly apparent only at high antibody concentrations (Figure 3B). Co-immunostaining with a mAb against calbindin-D28k confirmed Nedd4-2 immunostaining in calbindin-positive DCT and CNT and in calbindin-negative PT (Figure 3B).

Nedd4-2 Is Expressed in Segment-Specific and Intercalated Cells

The epithelium that lines the ASDN is heterogeneous and composed of segment-specific DCT, CNT, and CD cells and of intercalated cells (IC). The latter are subdivided further in proton-secreting type A IC with apical localization of vacuolar H^+-ATPase and bicarbonate-secreting type B IC with basolateral localization of H^+-ATPase (40). A third form (non-A–non-B) with diffuse labeling for the H^+-ATPase also is frequent in mice (40). Co-immunostaining for Nedd4-2 and vacuolar H^+-ATPase revealed that Nedd4-2 is highly abundant in the segment-specific ASDN cells and in IC with predominant basolateral and/or diffuse staining with the H^+-ATPase antibody (Figure 4), suggesting that among IC Nedd4-2 is predominantly expressed in non-A IC.

Quantitative RT-PCR and Western Blot Analysis Do not Detect Any Significant Effect of Altered Na^+ Intake on Nedd4-2 Expression in the Kidney

In heterologous expression systems, the cell surface density of ENaC is inversely correlated to the expression of Nedd4-2 (12,14,26). In rodents, high dietary Na^+ intake reduces and low dietary Na^+ intake increases the apical plasma membrane localization of ENaC (5,6). To test the hypothesis that dietary Na^+ intake may mediate its effects on the subcellular localization of ENaC by changes in the expression levels of Nedd4-2, we used first quantitative RT-PCR to determine Nedd4-2 expression levels in CD that were microdissected from the kidneys of mice on different Na^+ diets. The measured Nedd4-2 mRNA expression levels did not differ significantly between groups (99 ± 20 [high Na^+] *versus* 100 ± 12 arbitrary units [low Na^+], mean ± SEM; $P = 0.48$ [t test]; $n = 6$ mice per group; values were normalized to GAPDH and the low-Na^+ condition). Aldosterone-induced Sgk1 was significantly increased with dietary Na^+ restriction (22 ± 10 [high Na^+] *versus* 100 ± 13 arbitrary units [low Na^+], mean ± SEM; $P = 0.0003$; $n = 6$ mice per group; values were normalized to GAPDH and low Na^+), consistent with previous data (41) and confirming the validity of our RT-PCR method. Previous studies indicated that aldosterone may have an impact on the abundance of some proteins by posttranscriptional mechanisms. For example, it has been shown repeatedly that the expression of the thiazide-sensitive NaCl co-transporter is induced by aldosterone only at the protein but not at the mRNA level (42,43). To determine the effect of dietary Na^+ intake on Nedd4-2 protein levels, we performed immunoblotting with renal cortex homogenates from mice on different Na^+ diets. We did not detect significant difference in the abundance of Nedd4-2 protein between both groups of mice as demonstrated by densitometric quantification of protein bands that were obtained with the A26 antibody (10.9 ± 2.0 [high Na^+] *versus* 7.6 ± 1.0 arbitrary units [low Na^+], mean ± SEM; $n = 9$ mice per group; values were normalized to β-actin).

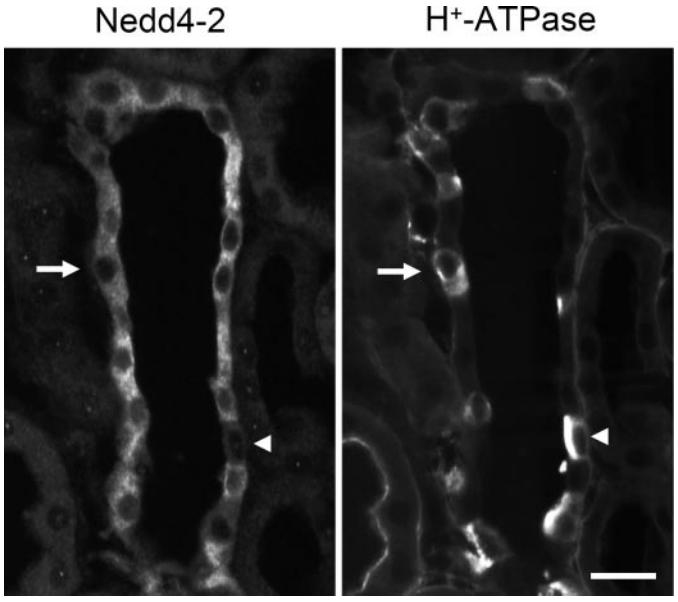

Figure 4. CCD profile in kidney of a mouse on a high sodium (Na^+) intake. Double immunofluorescence on the same cryostat section with affinity-purified rabbit anti–Nedd4-2 antiserum A26 and mouse mAb against vacuolar H^+-ATPase. Nedd4-2 immunostaining is seen in H^+-ATPase–negative principal cells and in some (arrow) but not all (arrowhead) H^+-ATPase–positive IC. The labeling of tubular basement membranes and interstitial cells in the right panel (H^+-ATPase) is due to binding of the secondary FITC-labeled anti-mouse IgG to endogenous immunoglobulins. Bar = approximately 20 μm.

Nedd4-2 Immunostaining Varies in Response to Altered Dietary Na^+ Intake and along the ASDN

PT contribute more than 70% to the fractional tubular volume of the renal cortex. It is conceivable that the "background" expression of Nedd4-2 in PT may prevent the detection of differences in Nedd4-2 expression in ASDN as long as tissue homogenates are analyzed. Therefore, we used immunohistochemistry to assess qualitatively the abundance of Nedd4-2 in the ASDN under the different conditions. In the kidneys of mice that were kept for 2 wk on a high dietary Na^+ intake, Nedd4-2 was easily detectable in the cytoplasm of all β-ENaC–positive CNT and CCD profiles. A low dietary Na^+ intake for 2 wk drastically reduced Nedd4-2 immunostaining in the ASDN segments. The intensity of Nedd4-2 immunostaining varied considerably along the ASDN segments. It was weak in late DCT and early CNT and increased progressively along the CNT and CCD. The axial heterogeneity of Nedd4-2 staining was seen with both Nedd4-2 antisera and is well evident when CNT and CD profiles are compared (Figure 5). The generally weak cytoplasmic Nedd4-2 immunostaining in some PT and distal tubules did not differ between mice that were on a low and a high dietary Na^+ intake (Figure 5).

Higher magnification of consecutive cryosections that were stained either with antibodies against ENaC or antibodies against Nedd4-2 demonstrated a close inverse corre-

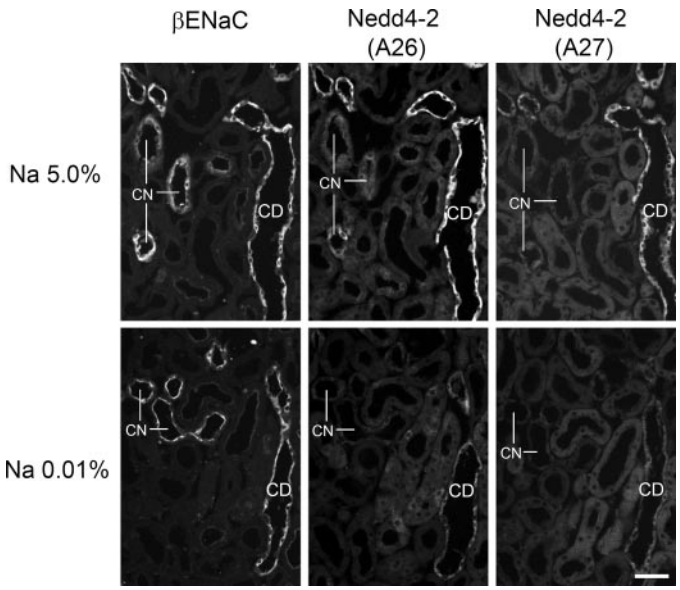

Figure 5. Overviews on renal cortex of mice that were kept for 2 wk on either a high-Na^+ (5%) or a low-Na^+ (0.01%) diet. Immunofluorescence with rabbit antisera against the β subunit of the epithelial Na^+ channel (β-ENaC) and Nedd4-2 (affinity-purified sera A26 and A27) on triplets of consecutive cryostat sections is shown. Compared with the situation on high Na^+ intake, dietary sodium restriction increases the apical localization of β-ENaC in connecting tubules (CN) and, although to less extent, in the CD, whereas it decreases the staining intensity with both Nedd4-2 antisera in the same tubules. Note the different Nedd4-2 staining intensity in CN and CD profiles. The weak cytoplasmic Nedd4-2 immunostaining in some proximal tubules (P) is not affected by dietary Na^+ intake. Bar = approximately 50 μm.

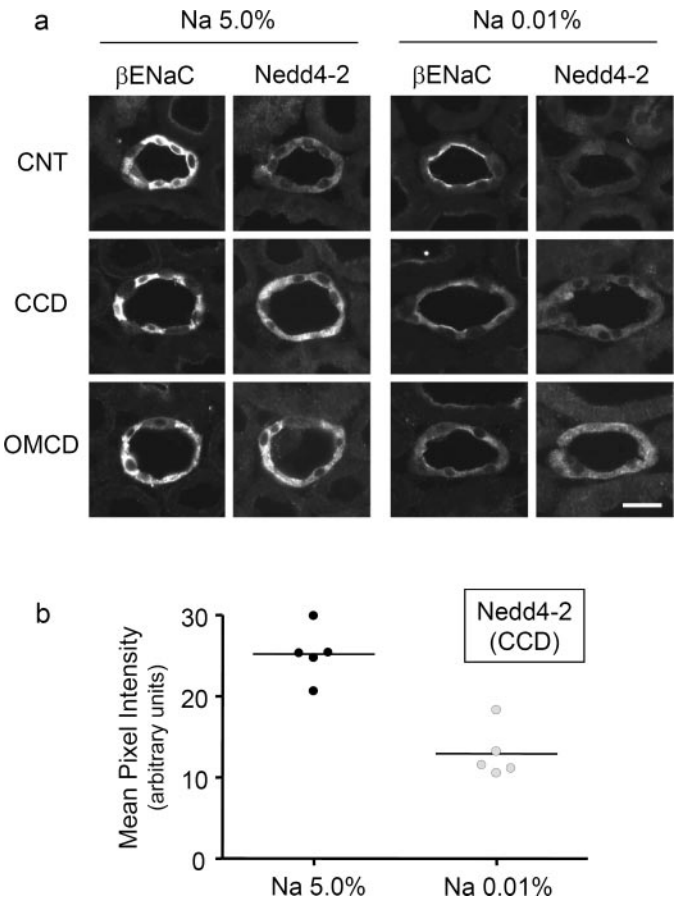

Figure 6. (A) CNT, CCD, and outer medullary CD (OMCD) profiles from mice that were kept for 2 wk on either a high-Na^+ (5%) or a low-Na^+ (0.01%) diet. Immunofluorescence with rabbit antisera against β-ENaC and Nedd4-2 (affinity-purified sera A26) on pairs of consecutive cryostat sections is shown. On a high Na^+ intake, β-ENaC is seen predominantly at intracellular sites in CNT, CCD, and OMCD, and Nedd4-2 immunostaining is strong in the same tubules. On a low Na intake, β-ENaC is shifted toward the apical plasma membrane, and Nedd4-2 immunostaining is decreased. Note the decreasing intensity of apical β-ENaC immunostaining from CNT to CD and the clear inverse relationship of apical ENaC localization and Nedd4-2, which is most evident on low-Na^+ diet. Bar = approximately 20 μm. (B) Mean pixel intensities (MPI) of Nedd4-2 immunostaining (affinity-purified sera A26) in CD of mice that were kept on the indicated sodium diets. At least three randomly selected CCD were analyzed per mouse as described (24). Each dot represents the MPI value for an individual mouse. The horizontal bars are the means for each group. The difference between the means is statistically significant ($P = 0.003$, unpaired t test).

lation between the apical localization of ENaC and the abundance of Nedd4-2 (Figure 6). On a high dietary Na^+ intake, β-ENaC was diffusely distributed within the cytoplasm of CNT, CCD, and outer medullary CD (OMCD) cells and Nedd4-2 was highly abundant in the cytoplasm of the epithelial cells of the same tubule. Dietary Na^+ restriction increased the apical localization of β-ENaC and significantly reduced the cytoplasmic immunostaining for Nedd4-2, when compared with the corresponding tubular segments of a mouse that was on a high-Na^+ diet. In mice that were on a low dietary Na^+ intake, apical localization of ENaC was most prominent in the CNT and decreased along the CCD toward the OMCD, whereas Nedd4-2 immunostaining exhibited an increasing gradient from CNT to OMCD (Figure 6A). The inverse correlation of apical ENaC localization and Nedd4-2 abundance also was seen in rats that were kept on a standard- or a low-Na^+ diet (Figure 7A), confirming that the diet changes of Nedd4-2 immunostaining are not species specific. The qualitative observations on altered Nedd4-2 immunostaining intensities in response to altered dietary Na^+ intake were substantiated further by measurements of MPI in Nedd4-2 immunostained CD (Figures 6B and 7B).

Intensity of Nedd4-2 Immunostaining Does not Depend on ENaC Activity

The data reported thus far support the hypothesis that dietary Na^+ restriction reduces Nedd4-2 expression in ASDN cells, which in turn may result in an enhanced cell surface abundance of ENaC. However, it also is conceivable that the increased Na^+ entry as a result of enhanced ENaC

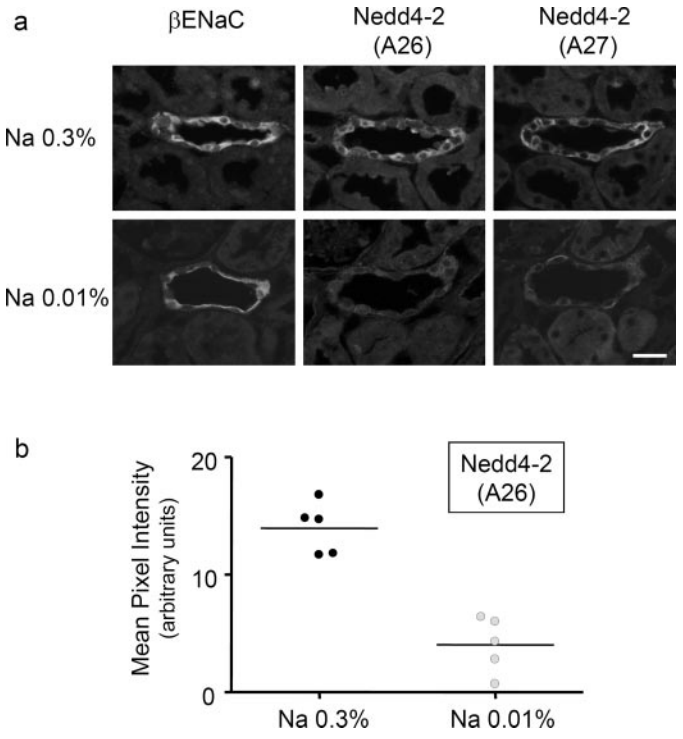

Figure 7. (A) CCD profiles from rats kept for 2 wk on either a standard-Na^+ (0.3%) or a low-Na^+ (0.01%) diet. Immunofluorescence with rabbit antisera against β-ENaC and Nedd4-2 (affinity-purified sera A26 and A27) on triplets of consecutive cryostat sections is shown. Note the predominant intracellular localization of β-ENaC, the strong cytoplasmic staining for Nedd4-2 on a standard Na^+ intake, the distinct apical localization of β-ENaC, and the weak staining for Nedd4-2 on a low Na^+ intake. Bar = approximately 20 μm. (B) MPI of Nedd4-2 immunostaining (affinity-purified sera A26) in CD of rats kept on the indicated sodium diets. At least three randomly selected CCD were analyzed per rat as described (24). Each dot represents the MPI value for an individual rat. The horizontal bars are the means for each group. The difference between the means is statistically significant ($P = 0.001$, unpaired t test).

activity is responsible for the reduced Nedd4-2 immunostaining in response to dietary Na^+ restriction. To test the latter hypothesis, we took advantage of a recently developed transgenic mouse line with targeted inactivation of α-ENaC in the CD (29). The loss of α-ENaC in the CD impairs the cell surface targeting of ENaC channels, and these mice consistently lack any ENaC activity in the apical plasma membrane of the CD. If the increased ENaC activity is responsible for the reduced Nedd4-2 expression, then we expected to see that lowered Na^+ intake reduces Nedd4-2 only in CD from wild-type mice but not in CD from transgenic mice. However, dietary Na^+ restriction similarly reduced Nedd4-2 immunostaining in CD profiles of mice of both genotypes (Figure 8). Therefore, apical ENaC activity seems not to interfere with the expression of Nedd4-2, as determined by immunohistochemistry.

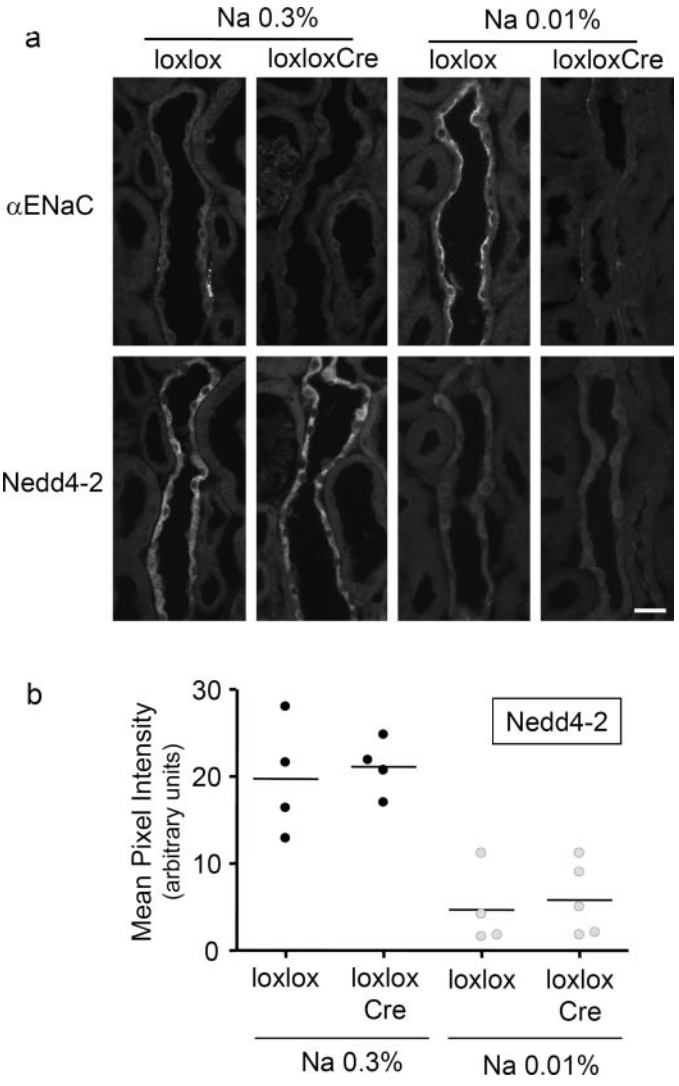

Figure 8. (A) CCD profiles from mice without ($Scnn1a^{loxlox}$) and with ($Scnn1a^{loxloxCre}$) targeted inactivation of α-ENaC in the CD. The generation and phenotypic characterization of these mice were described previously (29). Mice were kept either on standard-Na^+ diet (0.3%) or on dietary Na^+ restriction (Na^+ 0.01%) for 6 d. Immunofluorescence with rabbit antisera against α-ENaC and Nedd4-2 (affinity-purified sera A26) on pairs of consecutive cryostat sections is shown. Dietary Na^+ restriction induces α-ENaC and increases the apical localization α-ENaC in the $Scnn1a^{loxlox}$ mice, whereas α-ENaC is virtually absent from the CCD of the $Scnn1a^{loxloxCre}$ mice on both diets. Nedd4-2 immunostaining is well detectable in the CCD profiles of the mice on standard Na^+ (0.3%) intake and is similarly weak in the CCD profiles of mice of both genotypes on low-Na^+ diet. Bar = approximately 20 μm. (B) MPI of Nedd4-2 immunostaining (affinity-purified sera A26) in CD of mice of the four indicated experimental groups. At least three randomly selected CCD were analyzed per mouse as described (24). Each dot represents the MPI value for an individual mouse. The horizontal bars are the means for each group. Differences between diets but not between the genotypes for each diet were statistically significant (ANOVA followed by Bonferroni multiple comparisons test).

Long-Term Aldosterone Treatment Reduces Nedd4-2 Abundance in mpkCCD$_{cl4}$ Cells

Because ENaC activity does not regulate Nedd4-2 expression, we wondered whether it is aldosterone that affects Nedd4-2 expression. Chronic effects of aldosterone are difficult to analyze *in vivo*, because long-term treatment with aldosterone without any concomitant dietary Na^+ restriction causes extracellular volume expansion, hypokalemia, and alkalosis, which may confound the interpretation of results. We therefore chose an *in vitro* approach and stimulated mpkCCD$_{cl4}$ cells that were grown on collagen-coated filters for up to 5 d with aldosterone and followed the expression of Nedd4-2 by immunoblotting of cell lysates (Figure 9). When cells were cultured without aldosterone, Nedd4-2 remained constant. However, when aldosterone (1 μM) was added, a decrease in Nedd4-2 expression was observed starting at day 2 (Figure 9) and progressed up to day 5. The observed suppression of Nedd4-2 expression with aldosterone is consistent with the observed weak immunostaining for Nedd4-2 in animals with low-Na^+ diet, a condition in which plasma aldosterone is high.

Discussion

Our study provides a comprehensive analysis of the localization and regulation by dietary Na^+ intake of Nedd4-2 in rodent kidneys. We show that Nedd4-2 is expressed along the nephron, with the highest expression levels in ENaC-positive ASDN cells. Moreover, we reveal by immunohistochemistry a close reciprocal relationship of Nedd4-2 immunostaining intensity and apical ENaC localization in the kidney *in vivo*. This inverse relationship is seen both along the axis of the ASDN and in response to altered dietary Na^+ intake. Furthermore, we show by immunoblotting that long-term treatment with aldosterone downregulates Nedd4-2 protein levels in a mouse CCD cell line. Taken together with previous *in vitro* data, our study supports the hypothesis that Nedd4-2 is involved in the control of apical ENaC localization in the mammalian kidney.

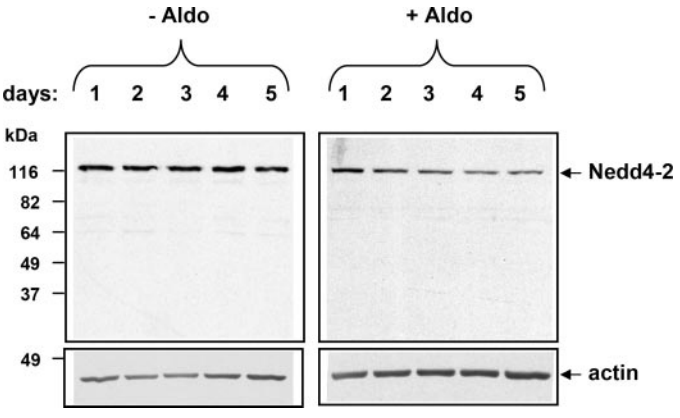

Figure 9. Immunoblot of mouse CCD mpkCCD cells that were treated for the indicated time intervals with either vehicle (−Aldo) or 1 μM aldosterone (+Aldo). Membranes were incubated with affinity-purified anti–Nedd4-2 antiserum A26 and subsequently probed with mouse anti–β-actin to confirm equal protein loading and transfer. For each lane, cells from three different filter cups were pooled. The shown blot is representative for the results from four independent experiments. Note the time-dependent decrease of Nedd4-2 protein abundance in aldosterone-treated cells that is not seen in vehicle-treated cells.

Nedd4-2 expression is found in various tissues and cell types, suggesting that Nedd4-2 has multiple cellular functions. Northern blot analysis revealed Nedd4-2 mRNA expression in brain, heart, lung, liver, and kidney (13,15,33). Within the human kidney, Nedd4-2 mRNA was reported to be expressed along the entire nephron (36). This study confirms these data for the mouse nephron and extends them to the protein level by demonstrating localization of Nedd4-2 protein in several tubular portions. The highest expression levels of Nedd4-2 protein were seen in ASDN segments, consistent with the proposed regulatory role of Nedd4-2 for ENaC function. However, Nedd4-2 also was seen in tubular segments that do not express ENaC. In particular, PT cells showed a considerable amount of Nedd4-2 mRNA expression and protein immunostaining. The functional role and the molecular targets for Nedd4-2 in non-ASDN tubular segments is unclear. The ClC5 Cl^- channels of PT and the β-subunit of the ClCk chloride channel of thick ascending limbs, barttin, were suggested to be putative targets for Nedd4-2 (44–46). ClC5 and barttin have PY motifs within their amino acid sequence, and in the *Xenopus* oocyte expression system, Nedd4-2 profoundly diminishes protein abundance and activity of co-expressed ClC5 and barttin *via* a PY motif–dependent mechanism (44–46).

Several previous *in vitro* experiments showed that Nedd4-2 decreases the abundance and activity of ENaC at the cell surface (12,14,26). Our study suggests that the same may hold true in the ASDN *in vivo*. As presented in Figures 4 through 7, we found a striking inverse relationship between the Nedd4-2 immunostaining intensity and the apical ENaC localization in ASDN cells of mice and rats. Whereas Nedd4-2 immunostaining increased along the axis of the ASDN, apical ENaC localization decreased. The axial gradient of apical ENaC localization was seen in several species and was evident also in microperfusion, micropuncture, and patch-clamp studies that showed much higher ENaC activity in early ASDN (*i.e.*, the CNT) than in late ASDN segments (*i.e.*, the CD) (2,7–11,29). Differences in the expression levels of mineralocorticoid receptor 11-βHSD2 and SGK1 likely do not account for this axial heterogeneity, because these ENaC-regulating molecules seem to be equally abundant along the CNT and CCD (reviewed in [(47]). To our knowledge, Nedd4-2 is the first known ENaC-regulatory protein that shows an axial gradient of expression along the ASDN that could help to explain the axial gradient of apical ENaC.

The close inverse relationship between Nedd4-2 immunostaining intensity and apical ENaC localization also was seen in response to altered dietary Na^+ intake, suggesting that changes in Nedd4-2 abundance contribute to the adaptation of ENaC cell surface activity to long-term changes in dietary Na^+ intake. Although quantitative RT-PCR with microdissected CCD and immunoblotting with kidney cortex homogenates failed to provide further conclusive support for this conclusion, the inverse correlation of Nedd4-2 immunostaining intensity and apical ENaC localization was observed consistently in mouse and rat

kidneys and was seen with two Nedd4-2 antibodies that were directed against two different, separated epitopes. This makes it unlikely but does not rule out that the observed changes in Nedd4-2 immunostaining intensities simply reflect altered Nedd4-2 conformations or protein–protein interactions that may limit access of the antibodies to the epitopes. While this article was in revision, Umemura *et al.* (48) found by using quantitative RT-PCR and *in situ* hybridization significantly higher Nedd4-2 mRNA expression levels in kidneys of Dahl salt-resistant rats that were kept on a 8% NaCl diet than in the kidneys of their littermates that were kept on a 0.3% NaCl diet. Although these results differ from our findings in mice, in which we did not see any apparent effect on Nedd4-2 mRNA levels, the data provide additional evidence that dietary Na^+ intake may have an impact on Nedd4-2 abundance. Remarkably, the authors also described that the diet-induced changes in Nedd4-2 mRNA expression were not observed in Dahl salt-sensitive rats, which led to the speculation that disturbed Nedd4-2 regulation in this model may contribute to the salt-sensitive phenotype of the rats.

It is interesting that dietary Na^+ restriction reduced Nedd4-2 immunostaining not only in the segment-specific ASDN cells but also in the IC. IC do not contribute directly to transepithelial Na^+ transport, indicated by the lack of ENaC expression (6) and the very low levels of Na^+-K^+-ATPase in their basolateral plasma membranes (49). IC are involved mainly in the urinary acidifying mechanism by secretion of protons (type A IC) or bicarbonate (type B IC). Moreover, they may limit renal K^+ loss as a result of K^+ reabsorption *via* an apical H^+,K^+-ATPase (50). Recent studies suggested that the non-A IC also may be important for transepithelial transport of Cl^- *via* pendrin, a Cl^-/HCO_3^- exchanger in the apical plasma membrane of these IC (51,52). Because dietary NaCl restriction equally reduces urinary Na^+ and Cl^+ excretion and because Nedd4-2 immunostaining is seen predominantly in the non-A IC, it is tempting to speculate that Nedd4-2 may have an impact on both Na^+ transport in the segment-specific DCT, CNT, and CD cells and Cl^- transport in IC, which would contribute to simultaneous maintenance of Na^+ and Cl^- balance.

What might be the underlying mechanism for the NaCl diet–induced changes in Nedd4-2 immunostaining? Our findings in mice, with targeted inactivation of α-ENaC in the CD, suggest that the observed changes in Nedd4-2 expression were not secondary to altered ENaC function. The findings in mpkC-CD_{cl4} cells rather suggested that long-term changes in aldosterone levels may regulate Nedd4-2 protein abundance. Remarkably, the downregulatory effect of aldosterone was apparent only after more than 1 d of aldosterone treatment, suggesting that changes in Nedd4-2 protein levels are not part of the early response to aldosterone. Consistent with these conclusions, we recently showed in the same CCD cell line and in kidneys of adrenalectomized rats that aldosterone does not change the level of Nedd4-2 protein within the first 2 h after aldosterone application (24). Within this early time frame, aldosterone, however, increased Nedd4-2 phosphorylation, which is thought to impair the interaction of Nedd4-2 with ENaC (see beginning of article). Taken together, these observations suggest a model in which the rapid effects of aldosterone on ENaC are mediated by phosphorylation of Nedd4-2, whereas the chronic effects of aldosterone involve altered Nedd4-2 protein levels. Whether the phosphorylation status of Nedd4-2 also may change with chronically altered Na^+ intake or aldosterone levels was not assessed in our study. Furthermore, the cellular and molecular mechanisms by which aldosterone modulates Nedd4-2 protein abundance and the role of other hormones that possibly are involved in the regulation of ENaC by dietary Na^+ intake (*e.g.*, angiotensin II) remain to be elucidated.

Conclusion

Our study shows a reciprocal relationship between Nedd4-2 immunostaining and apical ENaC localization along the ASDN. This study supports the important role of Nedd4-2 in renal Na^+ handling and suggests that aldosterone-dependent regulation of Nedd4-2 protein abundance may contribute to the long-term adaptation of apical ENaC activity to altered Na^+ transport requirements. Dysfunctions of these regulatory processes could either cause renal salt losing or predispose to salt-sensitive hypertension.

Acknowledgments

This work was supported by the Swiss National Science Foundation to O.S. (3100A0-103779/1) and to J.L. (3200B0-105769/1), the Roche Research Foundation in Basel (to O.S.), the Cloëtta Foundation (to J.L.), the EMDO Foundation (to J.L.), and the Swiss Diabetes Foundation (to J.L.). D.L.-C. is supported by a Marie-Heim Vögtlin Fellowship of the Swiss National Science Foundation.

We thank Drs. H. Abriel, D. Eladari, D. Firsov, J.-D. Horisberger, B. Kaissling, L. Schild, P. Shaw, and B. Rossier for comments on the manuscript and M. Carrel and M. Bloch-Faure for expert technical assistance. We are grateful to Dr. D. Ackermann and N. Gresko for valuable help with the microdissection of CCD from mice on different Na^+ diets. The ENaC antibodies and the kidneys from $Scnn1a^{loxlox}$ and $Scnn1a^{loxloxCre}$ were kindly provided by Drs. B. Rossier and E. Hummler. Samples of microdissected mouse glomeruli and renal tubules were from D. Firsov.

References

1. Bachmann S, Bostanjoglo M, Schmitt R, Ellison DH: Sodium transport-related proteins in the mammalian distal nephron: Distribution, ontogeny and functional aspects. *Anat Embryol (Berl)* 200: 447–468, 1999
2. Loffing J, Zecevic M, Feraille E, Kaissling B, Asher C, Rossier BC, Firestone GL, Pearce D, Verrey F: Aldosterone induces rapid apical translocation of ENaC in early portion of renal collecting system: Possible role of SGK. *Am J Physiol* 280: F675–F682, 2001
3. Verrey F, Hummler E, Schild L, Rossier, BC: Control of sodium transport by aldosterone. In: *The Kidney: Physiology and Pathophysiology*, 3rd Ed., edited by Seldin DW, Giebisch G, Philadelphia, Lippincott Williams & Wilkins, 2000, pp 1441–1471
4. Kellenberger S, Schild L: Epithelial sodium channel/degenerin family of ion channels: A variety of functions for a shared structure. *Physiol Rev* 82: 735–767, 2002
5. Masilamani S, Kim G-H, Mitchell C, Wade JB, Knepper MA: Aldosterone-mediated regulation of ENaC alpha,

beta, and gamma subunit proteins in rat kidney. *J Clin Invest* 104: R19–R23, 1999
6. Loffing J, Pietri L, Aregger F, Bloch-Faure M, Ziegler U, Meneton P, Rossier BC, Kaissling B: Differential subcellular localization of ENaC subunits in mouse kidney in response to high- and low-Na diets. *Am J Physiol* 279: F252–F258, 2000
7. Frindt G, Palmer LG: Na channels in the rat connecting tubule. *Am J Physiol Renal Physiol* 286: F669–F674, 2004
8. Costanzo LS: Comparison of calcium and sodium transport in early and late rat distal tubules: Effect of amiloride. *Am J Physiol* 246: F937–F945, 1984
9. Reif MC, Troutman SL, Schafer JA: Sodium transport by rat cortical collecting tubule. Effects of vasopressin and deoxycorticosterone. *J Clin Invest* 77: 1291–1298, 1986
10. Tomita K, Pisano JJ, Knepper MA: Control of sodium and potassium transport in the cortical collecting duct of the rat. Effects of bradykinin, vasopressin, and deoxycorticosterone. *J Clin Invest* 76: 132–136, 1985
11. Almeida AJ, Burg MB: Sodium transport in the rabbit connecting tubule. *Am J Physiol* 243: F330–F334, 1982
12. Abriel H, Loffing J, Rebhun JF, Pratt JH, Horisberger J-D, Rotin D, Staub O: Defective regulation of the epithelial Na+ channel (ENaC) by Nedd4 in Liddle's syndrome. *J Clin Invest* 103: 667–673, 1999
13. Kamynina E, Debonneville C, Bens M, Vandewalle A, Staub O: A novel mouse Nedd4 protein suppresses the activity of the epithelial Na+ channel. *FASEB J* 15: 204–214, 2001
14. Snyder PM, Steines JC, Olson DR: Relative contribution of Nedd4 and Nedd4-2 to ENaC regulation in epithelia determined by RNA interference. *J Biol Chem* 279: 5042–5046, 2004
15. Harvey KF, Dinudom A, Cook DI, Kumar S: The Nedd4-like protein KIAA0439 is a potential regulator of the epithelial sodium channel. *J Biol Chem* 276: 8597–8601, 2001
16. Debonneville C, Staub O: Participation of the ubiquitin-conjugating enzyme UBE2E3 in Nedd4-2-dependent regulation of the epithelial Na+ channel. *Mol Cell Biol* 24: 2397–2409, 2004
17. Staub O, Gautschi I, Ishikawa T, Breitschopf K, Ciechanover A, Schild L, Rotin D: Regulation of stability and function of the epithelial Na+ channel (ENaC) by ubiquitination. *EMBO J* 16: 6325–6336, 1997
18. Pisitkun T, Shen RF, Knepper MA: Identification and proteomic profiling of exosomes in human urine. *Proc Natl Acad Sci U S A* 101: 13368–13373, 2004
19. Hansson JH, Nelson-Williams C, Suzuki H, Schild L, Shimkets RA, Lu Y, Canessa CM, Iwasaki T, Rossier BC, Lifton RP: Hypertension caused by a truncated epithelial sodium channel gamma subunit: Genetic heterogeneity of Liddle syndrome. *Nat Genet* 11: 76–82, 1995
20. Shimkets RA, Warnock DG, Bositis CM, Nelson-Williams C, Hansson JH, Schambelan M, Gill JR, Ulick S, Milora RV, Findling JW, Canessa CM, Rossier BC, Lifton RP: Liddle's syndrome: Heritable human hypertension caused by mutations in the beta subunit of the epithelial sodium channel. *Cell* 79: 407–414, 1994
21. Naray-Fejes-Toth A, Canessa CM, Cleaveland ES, Aldrich G, Fejes-Toth G: sgk is an aldosterone-induced kinase in the renal collecting duct. *J Biol Chem* 274: 16973–16978, 1999
22. Chen S, Bhargava A, Mastroberardino L, Meijer OC, Wang J, Buse P, Firestone GL, Verrey F, Pearce D: Epithelial sodium channel regulated by aldosterone-induced protein sgk. *Proc Natl Acad Sci U S A* 96: 2514–2519, 1999
23. Faletti CJ, Perrotti N, Taylor SI, Blazer-Yost BL: sgk: An essential convergence point for peptide and steroid hormone regulation of ENaC-mediated Na+ transport. *Am J Physiol* 282: C494–C500, 2002
24. Flores SY, Loffing-Cueni D, Kamynina E, Daidie D, Gerbex C, Chabanel S, Dudler J, Loffing J, Staub O: Aldosterone-induced serum and glucocorticoid-induced kinase 1 expression is accompanied by Nedd4-2 phosphorylation and increased Na+ transport in cortical collecting duct cells. *J Am Soc Nephrol* 16: 2279–2287, 2005
25. Snyder PM, Olson DR, Thomas BC: Serum and glucocorticoid-regulated kinase modulates Nedd4-2-mediated inhibition of the epithelial Na+ channel. *J Biol Chem* 277: 5–8, 2002
26. Debonneville C, Flores SY, Kamynina E, Plant PJ, Tauxe C, Thomas MA, Munster C, Chraibi A, Pratt JH, Horisberger JD, Pearce D, Loffing J, Staub O: Phosphorylation of Nedd4-2 by Sgk1 regulates epithelial Na(+) channel cell surface expression. *EMBO J* 20: 7052–7059, 2001
27. Bhalla V, Daidie D, Li H, Pao AC, Lagrange LP, Wang J, Vandewalle A, Stockand JD, Staub O, Pearce D: Serum- and glucocorticoid-regulated kinase 1 regulates ubiquitin ligase neural precursor cell-expressed, developmentally down-regulated protein 4-2 by inducing interaction with 14-3-3. *Mol Endocrinol* 19: 3073–3084, 2005
28. Ichimura T, Yamamura H, Sasamoto K, Tominaga Y, Taoka M, Kakiuchi K, Shinkawa T, Takahashi N, Shimada S, Isobe T: 14-3-3 proteins modulate the expression of epithelial Na+ channels by phosphorylation-dependent interaction with Nedd4-2 ubiquitin ligase. *J Biol Chem* 280: 13187–13194, 2005
29. Rubera I, Loffing J, Palmer LG, Frindt G, Fowler-Jaeger N, Sauter D, Carroll T, McMahon A, Hummler E, Rossier BC: Collecting duct-specific gene inactivation of alphaENaC in the mouse kidney does not impair sodium and potassium balance. *J Clin Invest* 112: 554–565, 2003
30. Elalouf JM, Buhler JM, Tessiot C, Bellanger AC, Dublineau I, de Rouffignac C: Predominant expression of beta 1-adrenergic receptor in the thick ascending limb of rat kidney. Absolute mRNA quantitation by reverse transcription and polymerase chain reaction. *J Clin Invest* 91: 264–272, 1993
31. Chomczynski P, Sacchi N: Single-step method of RNA isolation by acid guanidinium thiocyanate-phenol-chloroform extraction. *Anal Biochem* 162: 156–159, 1987
32. Bens M, Vallet V, Cluzeaud F, Pascual-Letallec L, Kahn A, Rafestin-Oblin ME, Rossier BC, Vandewalle A: Corticosteroid-dependent sodium transport in a novel immortalized mouse collecting duct principal cell line. *J Am Soc Nephrol* 10: 923–934, 1999
33. Kamynina E, Tauxe C, Staub O: Differential characteristics of two human Nedd4 proteins with respect to epithelial Na+ channel regulation. *Am J Physiol* 281: F469–F477, 2001
34. Hemken P, Guo XL, Wang ZQ, Zhang K, Gluck S: Immunologic evidence that vacuolar H+ ATPases with heterogeneous forms of Mr = 31,000 subunit have different membrane distributions in mammalian kidney. *J Biol Chem* 267: 9948–9957, 1992
35. Auberson M, Hoffmann-Pochon N, Vandewalle A, Kellenberger S, Schild L: Epithelial Na+ channel mutants causing

Liddle's syndrome retain ability to respond to aldosterone and vasopressin. *Am J Physiol* 285: F459–F471, 2003
36. Chabardes-Garonne D, Mejean A, Aude J-C, Chevel L, Di Stefano A, Gaillard M-C, Imbert-Teboul M, Wittner M, Balian C, Anthouard V, Robert C, Segurens B, Wincker P, Weissenbach J, Doucet A, Elalouf JM: A panoramic view of gene expression in the human kidney. *Proc Natl Acad Sci U S A* 100: 13710–13715, 2003
37. Dunn DM, Ishigami T, Pankow J, Von Niederhausern A, Alder J, Hunt SC, Leppert MF, Lalouel JM, Weiss RB: Common variant of human NEDD4L activates a cryptic splice site to form a frameshifted transcript. *J Hum Genet* 47: 665–676, 2002
38. Itani OA, Campbell JR, Herrero J, Snyder PM, Thomas CP: Alternative promoter usage and differential splicing leads to human Nedd4-2 isoforms with a C2 domain and with variable number of WW domains. *Am J Physiol* 285: F916–F929, 2003
39. Chen H, Ross CA, Wang N, Huo Y, MacKinnon DF, Potash JB, Simpson SG, McMahon FJ, DePaulo JR Jr, McInnis MG: NEDD4L on human chromosome 18q21 has multiple forms of transcripts and is a homologue of the mouse Nedd4-2 gene. *Eur J Hum Genet* 9: 922–930, 2001
40. Kim J, Kim YH, Cha JH, Tisher CC, Madsen KM: Intercalated cell subtypes in connecting tubule and cortical collecting duct of rat and mouse. *J Am Soc Nephrol* 10: 1–12, 1999
41. Hou J, Speirs HJ, Seckl JR, Brown RW: Sgk1 gene expression in kidney and its regulation by aldosterone: Spatiotemporal heterogeneity and quantitative analysis. *J Am Soc Nephrol* 13: 1190–1198, 2002
42. Masilamani S, Wang X, Kim GH, Brooks H, Nielsen J, Nielsen S, Nakamura K, Stokes JB, Knepper MA: Time course of renal Na-K-ATPase, NHE3, NKCC2, NCC, and ENaC abundance changes with dietary NaCl restriction. *Am J Physiol Renal Physiol* 283: F648–F657, 2002
43. Abdallah JG, Schrier RW, Edelstein C, Jennings SD, Wyse B, Ellison DH: Loop diuretic infusion increases thiazide-sensitive Na(+)/Cl(−)-cotransporter abundance: Role of aldosterone. *J Am Soc Nephrol* 12: 1335–1341, 2001
44. Embark HM, Bohmer C, Palmada M, Rajamanickam J, Wyatt AW, Wallisch S, Capasso G, Waldegger P, Seyberth HW, Waldegger S, Lang F: Regulation of CLC-Ka/barttin by the ubiquitin ligase Nedd4-2 and the serum- and glucocorticoid-dependent kinases. *Kidney Int* 66: 1918–1925, 2004
45. Schwake M, Friedrich T, Jentsch TJ: An internalization signal in ClC-5, an endosomal Cl-channel mutated in dent's disease. *J Biol Chem* 276: 12049–12054, 2001
46. Hryciw DH, Ekberg J, Lee A, Lensink IL, Kumar S, Guggino WB, Cook DI, Pollock CA, Poronnik P: Nedd4-2 functionally interacts with ClC-5: Involvement in constitutive albumin endocytosis in proximal tubule cells. *J Biol Chem* 279: 54996–55007, 2004
47. Loffing J, Kaissling B: Sodium and calcium transport pathways along the mammalian distal nephron: From rabbit to human. *Am J Physiol Renal Physiol* 284: F628–F643, 2003
48. Umemura M, Ishigami T, Tamura K, Sakai M, Miyagi Y, Nagahama K, Aoki I, Uchino K, Rohrwasser A, Lalouel JM, Umemura S: Transcriptional diversity and expression of NEDD4L gene in distal nephron. *Biochem Biophys Res Commun* 339: 1129–1137, 2006
49. Sabolic I, Herak-Kramberger CM, Breton S, Brown D: Na/K-ATPase in intercalated cells along the rat nephron revealed by antigen retrieval. *J Am Soc Nephrol* 10: 913–922, 1999
50. Silver RB, Choe H, Frindt G: Low-NaCl diet increases H-K-ATPase in intercalated cells from rat cortical collecting duct. *Am J Physiol* 275: F94–F102, 1998
51. Quentin F, Chambrey R, Trinh-Trang-Tan MM, Fysekidis M, Cambillau M, Paillard M, Aronson PS, Eladari D: The Cl−/HCO3− exchanger pendrin in the rat kidney is regulated in response to chronic alterations in chloride balance. *Am J Physiol Renal Physiol* 287: F1179–F1188, 2004
52. Verlander JW, Hassell KA, Royaux IE, Glapion DM, Wang ME, Everett LA, Green ED, Wall SM: Deoxycorticosterone upregulates PDS (Slc26a4) in mouse kidney: Role of pendrin in mineralocorticoid-induced hypertension. *Hypertension* 42: 356–362, 2003